Materials Letters: X 15 (2022) 100161

Contents lists available at ScienceDirect

Materials Letters: X

journal homepage: www.sciencedirect.com/journal/materials-letters-x

On the nanoindentation behavior of a TiC layer formed through thermo-reactive diffusion during hot pressing of Ti and cast iron

Marius Grad [a,b,*], Naresh Nadammal [a,b], Darius Tytko [c], Ulf Noster [a,b]

[a] Ostbayerische Technische Hochschule (OTH) Regensburg, Galgenbergstrasse 30, Germany
[b] Technologie Campus Parsberg-Lupburg, Am Campus 1, Parsberg, Germany
[c] TESCAN GmbH, Zum Lonnenhohl 46, 44319 Dortmund, Germany

ARTICLE INFO

Keywords:
Hot pressing
Titanium alloys
Hard coating
Nanoindentation
Electron backscatter diffraction

ABSTRACT

Hot pressing of pure Ti and cast iron under vacuum formed a ~15 μm wide TiC-layer through the thermo-reactive diffusion process. Nanoindentation testing of the TiC-layer revealed average hardness and elastic modulus values of ~35 GPa and ~400 GPa, respectively. High-resolution indentation mapping indicated hardness change across the boundary with peak values observed within the TiC-layer. Solid state high temperature diffusion holds significant potential for developing uniform hard coatings on pure Ti/Ti-alloys.

Introduction

Despite specific advantages such as good strength to weight ratio and high corrosion resistance, inferior surface characteristics of Ti and its alloys limit their use in critical applications where the contact between other hard metallic materials are involved [1]. A crucial step in overcoming this issue is to enhance the surface properties of Ti and Ti-alloys by forming uniform protective hard coatings by physical and chemical vapor deposition [2–6]. However, the deposited coatings are usually thin, and the time required for deposition are quite high making these methods suitable only for small-scale critical applications.

Hot pressing (HP) [7] is a rather simple procedure in which pure Ti/Ti-alloys are bonded together in the solid form with an alloy containing a minimum of 0.2 wt% C (for TiC). This is followed by holding the material combination in a furnace at a specific temperature which is usually above the beta transus (882 °C/1155 K) of Ti due to the higher diffusion coefficient of C in β-Ti than in α-Ti. Thermo-reactive diffusion is followed by doing so leading to the formation of a TiC layer with a minimum thickness of 5 μm [8]. Thus, HP holds enormous potential to enhance the surface properties of Ti and Ti alloys.

Zhao et al. [9] proposed contact solid carburization to fabricate TiC coatings on top of Ti alloys using cast iron as a carbon sponge. A dense coating comprising equi-axed grains with a hardness of 2400 $HV_{0.05}$ and excellent adhesive strength was reported in their study. Sequential carburization was attempted by Luo et al. [10] to fabricate a Ti cermet on top of Ti6Al4V alloy. Significant improvement in the hardness and fracture toughness was reported by the authors together with a plasticity of ~32 %. Kvashina et al. [11] reported the formation of TiC by low temperature and very low pressure sintering of a mixture consisting pure titanium and graphite powders in a HP plant. The initial mixture was mechanically treated in a ball mill under an argon gas medium using steel balls prior to sintering.

The distinct experimentation routes establish the possibilities of HP as a potential method to fabricate TiC coatings on Ti/Ti-alloys. Even with the successful of deposition of such coatings through HP, characterization and testing of these coatings persists as a concern due to the narrow width and the composition variation observed across the starting materials. Thus, it is of critical importance to combine characterization and testing methods that delivers statistically significant information. Therefore, nanoindentation was combined with energy dispersive X-ray spectroscopy (EDS) and electron back-scatter diffraction (EBSD) in this study to evaluate the coatings formed through HP.

Materials and methods

Commercially pure titanium grade 2 (CP-Ti-2) and spheroidal graphite cast iron (SGCI) with 2.06 wt% C were used as the starting materials for HP. The specimens were pressed together using a *T*-clamp and heat treated at a temperature of 1050 °C for 3 h in a Linn High vacuum furnace. The HP temperature was thus kept below the melting temperature of SGCI.

A TESCAN Clara field emission scanning electron microscope was

* Corresponding author.
E-mail address: marius.grad@oth-regensburg.de (M. Grad).

https://doi.org/10.1016/j.mlblux.2022.100161
Received 4 June 2022; Accepted 20 July 2022
Available online 27 July 2022

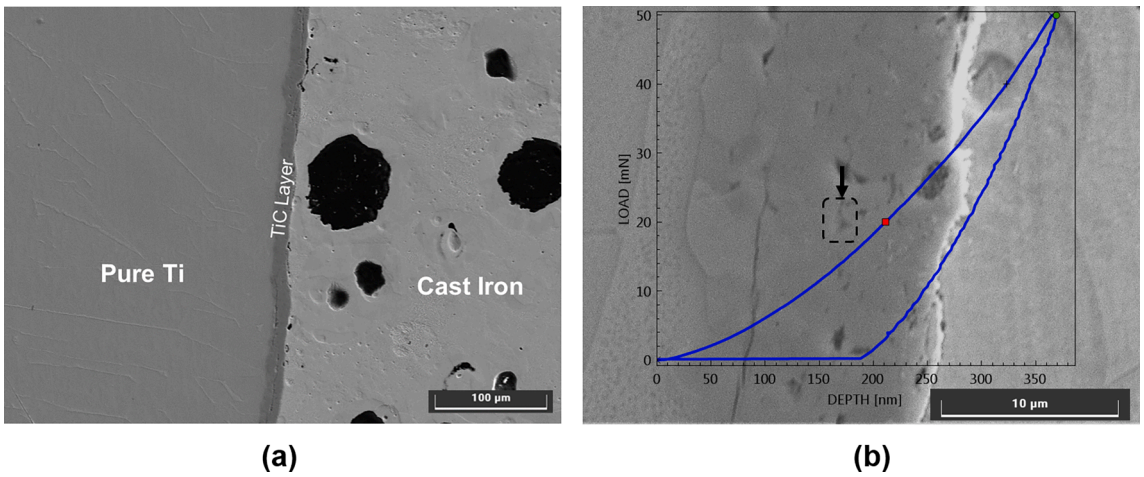

Fig. 1. (a) An overview SE image representing the formation of TiC layer (b) load-depth curve from a single indentation with the arrow mark indicating the location of indentation.

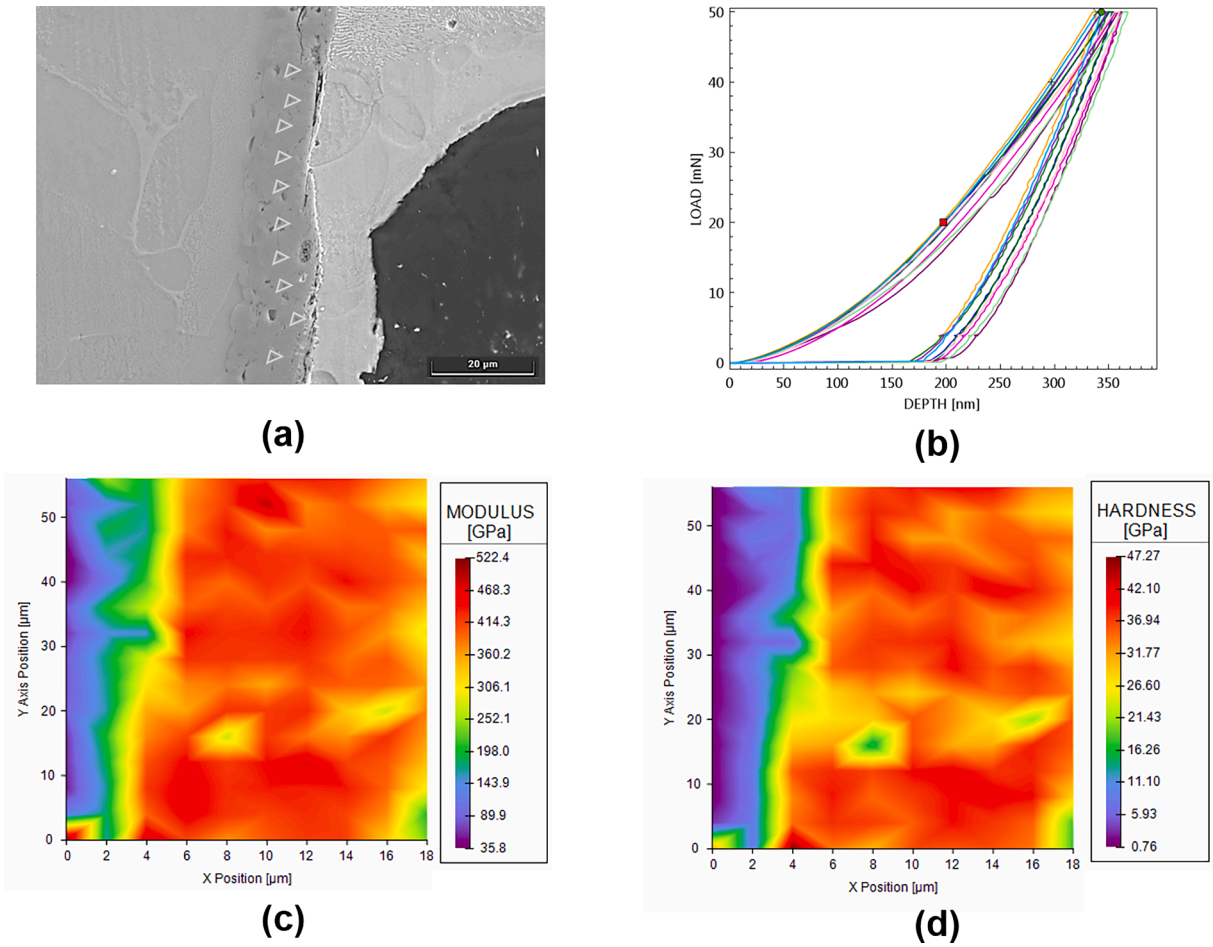

Fig. 2. (a) SE image representing the location of the ten indentation measurements (b) load vs depth plot of the ten indentations (c) modulus and (d) hardness mapping within the TiC layer.

used for the microscopic analysis. An Octane Elect EDS detector was used for the elemental composition analysis. A Velocity Pro detector was used for the EBSD analysis of the TiC layer and starting materials.

Nanoindentation experiments were performed in-situ using a NanoFlip InForce 50 Nanoindenter. The objective of the nano-indentation testing was to evaluate the hardness and the elastic modulus of TiC coating. A Berkovich-type diamond indentation tip was used for the testing. The whole nanoindentation set-up was assembled inside the TESCAN Clara SEM prior to testing. Poisson ratio of TiC was taken from the literature as 0.185 [12] for measuring the elastic modulus. Single and multiple indentation tests were performed within the TiC layer using a maximum force of 50 mN and a constant strain rate of 0.002 s^{-1}.

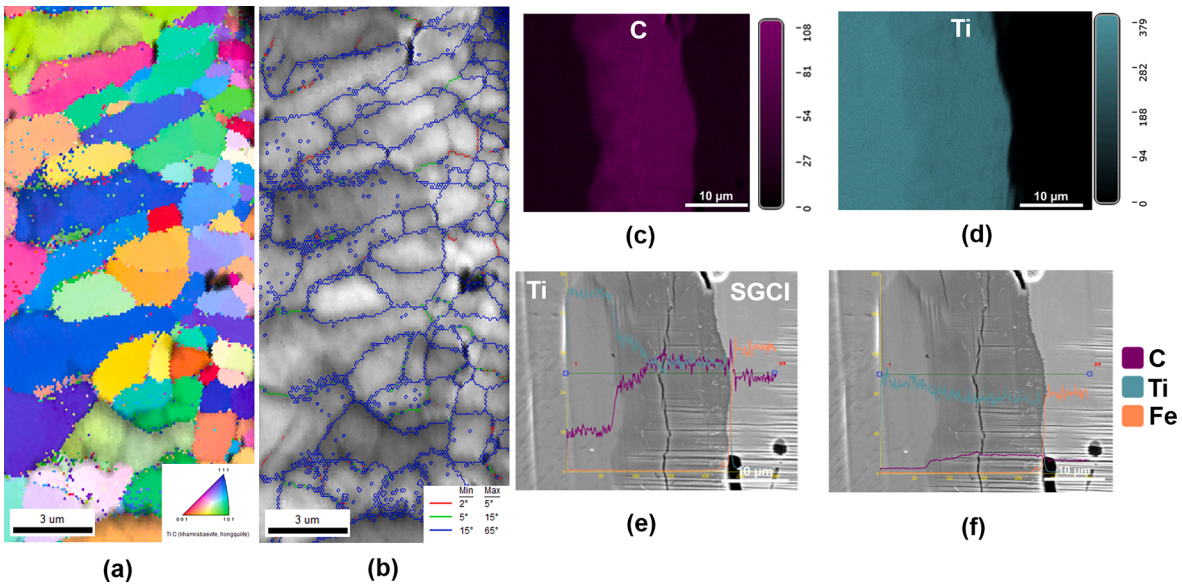

Fig. 3. (a) EBSD generated IPF map (b) grain boundary super-imposed image quality map (c-d) EDS area mapping with the Ti and C concentration, (e) atomic percentage & (f) weight percentage line scan profile from Ti to SGCI.

Results and discussion

A secondary electron (SE) image representing the diffusively formed TiC layer between Ti and SGCI is shown in Fig. 1a. A single indentation performed on the TiC layer is highlighted using an arrow and the associated load-depth curve is depicted in Fig. 1b. It can be noted that for the maximum load of 50 mN, the depth of indentation was around 370 nm only. From the total depth of 370 nm, ~170 nm depth was recovered when the indenter was removed from the sample. Load-depth curve indicates the elastic–plastic deformation under the influence of the nanoindenter. Corresponding hardness and E-modulus values were ~33 GPa and ~432 GPa, respectively.

A further confirmation on the formation of a hard and stiff TiC layer was obtained by making ten indents in the form of a vertical array. Even at higher useful magnifications, the indentations were hardly visible due to the huge amount of elastic recovery observed within the TiC layer. The load-depth and hardness-depth curves for the ten indentations is shown in Fig. 2a&b, respectively. It can be noted that both the plots reveal overlapping data points for the ten indentations suggesting the formation of a uniform TiC layer formation. The average hardness and modulus values from the further evaluation of ten indentations were ~36 GPa and ~490 GPa, respectively. A high-resolution indentation mapping performed on the TiC layer is shown in Fig. 2c&d. It is worth noting that the modulus and hardness profiles were both consistent, indicating the formation of a uniform TiC layer having a width of ~15 µm.

EBSD generated inverse pole figure (IPF) and grain boundary super-imposed image quality (IQ) maps are shown in Fig. 3a&b, respectively. A gradient in the grain size can be observed in both maps with smaller grains observed close to the SGCI. EDS area mapping revealing the distribution of Ti and C within the boundary region between pure Ti and SGCI is shown in Fig. 3c&d. Within the TiC layer, a uniform distribution of C can be observed with an associated decline in the Ti intensity in comparison with that detected for pure Ti. To further validate the formation of a wide TiC layer, line scans based on atomic and weight percentages were carried out across the boundary from Ti to SGCI and shown in Fig. 3d&e, respectively. Equi-atomic distribution of Ti and C can be observed starting at the boundary separating TiC and SGCI until three-fourth the width of the TiC layer. This is followed by a slight decrease in the C concentration and the corresponding increase in Ti concentration close to the boundary separating TiC layer and pure Ti. Atomic weight of Ti being approximately-four times higher than that of C, the weight percent scan reveals this difference explicitly. The preferential formation of a stoichiometric TiC in a Ti-C-Fe system by the suppression of FeTi and Fe_2Ti phases is due to the stronger bonding capacity of C with Ti and the order of standard free energy of formation which is TiC < Fe_2Ti < FeTi [13–14]. This indicates that TiC is the most easily formed phase at the Ti/ SGCI interface. In addition to that, the formed TiC layer acts as a further barrier for the diffusion of Fe atoms across the interface [15–16].

Surface property improvements through the deposition of strong and hard coatings are required for the wider application range of Ti and Ti-alloys. A diverse application range of Ti and Ti-alloys necessitates a cost-effective technology for the fabrication of hard surface layers. HP is an economical way to achieve the necessary objectives of a uniform, thick and hard layer on top of Ti and Ti alloys to improve their surface performance. The formation of a uniform layer was established using the load-depth curves as well as through the high-resolution hardness and elastic modulus mapping. The activation energy required for surface diffusion being substantially lower than that required for lattice and grain boundary diffusion processes giving HP a major advantage over the other approaches. In addition to that, the involved high temperature vacuum treatment further aids the surface diffusion by lowering the activation energy.

Enormous possibilities exist for the optimization of process parameters to further improve the quality of formed hard TiC coatings. In addition to that, the high hardness and elastic modulus of TiC layer is expected to enhance the surface properties of Ti alloys. Therefore, the next steps in the ongoing research investigations are to carry out the wear testing of TiC layer and its performance comparison with pure Ti.

Declaration of Competing Interest

The authors declare that they have no known competing financial interests or personal relationships that could have appeared to influence the work reported in this paper.

References

[1] H. Dong: Metals and Surface Engineering, UK, 27 March 2014, pp. 58-80.
[2] D. He, S. Zheng, P.u. Jibin, G. Zhang, H.u. Litian, Tribology international 82 (2015) 20–27.

[3] S. Zhang, F. Yan, Y. Yang, M. Yan, Y. Zhang, J. Guo, H. Li, Applied Surface Science 488 (2019) 61–69.
[4] E. Marin, R. Offoiach, M. Regis, S. Fusi, A. Lanzutti, L. Fedrizzi, Materials & Design 89 (2016) 314–322.
[5] T. Grögler, O. Plewa, S.M. Rosiwal, R.F. Singer, International journal of refractory metals and hard materials 16 (3) (1998) 217–222.
[6] Y.F.Z.Y. Cheng, Y.F. Zheng, Surface and Coatings Technology 201 (9–11) (2007) 4909–4912.
[7] Z. Zhao, P. Hui, F. Liu, L. Zhong, M. Zhao, B.o. Li, F. Yan, L.u. Zhengxin, Y. Ding, X. u. Yunhua, Journal of Alloys and Compounds 817 (2020), 152725.
[8] J. Zhang, S. Li, L.u. Chenfeng, C. Sun, P.u. Shuai, Q.i. Xue, Y. Lin, M. Huang, Surface and Coatings Technology 364 (2019) 265–272.
[9] Z. Zhao, P. Hui, X.u. Tao Wang, Y.X. Wang, Journal of Alloys and Compounds 745 (2018) 637–643.
[10] Y. Luo, H. Jiang, G. Cheng, H. Liu, Journal of Bionic Engineering 8 (1) (2011) 86–89.
[11] T. Kvashina, N. Uvarov, A. Ukhina, Ceramics 3 (3) (2020) 306–311.
[12] M. Sribalaji, Aminul Islam, Biswajyoti Mukherjee, Mayank Kumar Pandey, Ceramics International 44 (2) (2018) 2552–2562.
[13] N. Frage, L. Levin, E. Manor, R. Shneck, J. Zabicky, Scripta materialia 35 (7) (1996) 791–797.
[14] N. Frage, L. Levin, E. Manor, R. Shneck, J. Zabicky, Scripta materialia 35 (7) (1996) 799–803.
[15] B. Li, Zejun Chen, Weijun He, Ting Zhou, Ying Wang, Lin Peng, Jun Li, Qing Liu, Materials Characterization 148 (2019) 243–251.
[16] X. Yang, Kai Guo, Yunzhe Gao, Wu Bingnan, Jian Li, Yuwei Gao, Qingfeng Wang, Fucheng Zhang, Materials Science and Engineering: A 824 (2021), 141802.